Modification of Bovine Pancreatic Ribonuclease A with the Site-Specific Reagent 4-Arsono-2-nitrofluorobenzene. Spectrophotometric Titration of Arsononitrophenyl Ribonuclease A Derivatives†

Charles F. Hummel, Bernard R. Gerber, Anthony M. Babich, Matthew J. Avitable, and Robert P. Carty*

ABSTRACT: The 4-arsono-2-nitrophenyl chromophore can serve as a versatile spectrophotometric probe of the surface structure of proteins. Values of pK_1' and pK_2' for the arsonic acid ionizations are near 3 and 8, respectively, and the presence of nearby positive and negative charges produces substantial alterations in the spectral response of the probe. Changes in the extinction at the wavelength of maximum difference are 30–50% of the extinction coefficients, ϵ_{max}, for each ionization of the arsonic acid moiety. The titration of 41-(4-arsono-2-nitrophenyl) ribonuclease A indicates that the arsonate dianion binds near the active-site histidine residues. With protonation of a carboxylate side chain in the acidic region, presumably aspartic acid-121, the active site is disrupted. The 41-(4-arsono-2-nitrophenyl) group interacts to a greater degree with the histidine-119 side chain than it does with the histidine-12 residue. Interactions of uridine or 3′-cytidylic acid with the ligand-binding region of 41-(4-arsono-2-nitrophenyl) ribonuclease A modify the spectrophotometric response extensively. 3′-Cytidylic acid binds 41-(4-arsono-2-nitrophenyl) ribonuclease A with an affinity 300 times less than that for native ribonuclease A and 17 times lower than that for 41-(2,4-dinitrophenyl) ribonuclease A. The arsononitrophenyl chromophore is responsive to changes in the active site of ribonuclease A induced by such perturbants as ligand binding, chemical modification, and both acid and thermal denaturation.

Spectroscopic probes responsive to visible radiation monitor the surface conformation of proteins under a variety of conditions (Klotz & Tosi, 1962; Burr & Koshland, 1964; Naik & Horton, 1973). Reporter groups sensitive to pH and ligand binding (Kagan & Vallee, 1969), solvent perturbation (Ettinger & Hirs, 1968), transition from solution to the crystalline state (Johansen & Vallee, 1971), and protein–protein interactions (Tawada et al., 1969; Yagisawa, 1975) have been explored. The arsanilazo group characterizes the binding of substrate and product molecules to carboxypeptidase A and isomerization of the enzyme–ligand complex (Harrison & Vallee, 1978). 2-Mercuri-4-nitrophenol delineates kinetic and structural features associated with the binding of the inducer, isopropyl β-D-thiogalactoside, to the lactose repressor protein of *Escherichia coli* (Yang & Matthews, 1976; Friedman et al., 1976).

Spectroscopic probes show specificity of reaction with usually one or a few types of protein side chains (Horton & Koshland, 1967, 1972). Ideally, a probe of a protein surface should react at a single residue. When a probe is introduced at two or more sites, the spectrophotometric response is an average of conformational effects occurring in the environments of these sites (Garel & Baldwin, 1975; Friedman et al., 1976). Some reporter groups show marked differential kinetic reactivity for individual functional groups within a given residue class. 41-DNP RNase A[1] could be prepared by the selective arylation of the Lys-41 residue (Hirs et al., 1962, 1965; Hirs & Kycia, 1965). Equilibrium binding of 3′-CMP to 41-DNP RNase A was monitored in the visible region of the DNP spectrum (Ettinger & Hirs, 1968). Structural changes in RNase A with thermal unfolding, ligand binding, and isomerization at pH 6 are observable by using the fluoresceinthiocarbamoyl group (Garel, 1976).

4-Arsono-2-nitrofluorobenzene, ANFB, reacts selectively with the 1-α- and 41-amino groups of RNase A (unpublished experiments). The predominant reaction with the 41-amino group is partially governed by the dianionic character of the arsonate moiety at pH 8 (Kortum et al., 1961) and the presence of an anion-binding site in the enzyme (Wyckoff et al., 1970). Such selectivity might be demonstrable for other proteins and enzymes with anion-binding sites containing lysine side chains (Muhlrad et al., 1975). Hence, an examination of the spectrophotometric properties of the ANP group in monosubstituted RNase A derivatives and the effect of the usual protein perturbants on this visible chromophore was initiated.

Materials and Methods

Proteins. 41-ANP RNase A, 1-α-ANP RNase A, performic acid oxidized 41-ANP RNase A, *N*-3-CM-His-12 41-ANP RNase A, and *N*-1-CM-His-119 41-ANP RNase A (unpublished experiments), and 41-SNP RNase A were made as previously described (Carty & Hirs, 1968).

Model Compounds. (*A*) *ANP-glycinamide.* ANFB (1.32 g, 5 mmol) and glycinamide hydrochloride (0.55 g, 5 mmol) were dissolved in 50 mL of 1 M triethylammonium bicarbonate, pH 8.15. After 143 h at 25 °C, the solution was evaporated to dryness, coevaporated with MeOH and EtOH, and dried. The residue was taken up in water, titrated to pH 2 with 12 N HCl, evaporated to dryness, and crystallized from hot water to yield 760 mg (48%) of product: vis_{max} (0.2 M sodium phosphate, pH 6) 410 nm (ε 5620), vis_{min} 318 nm (ε 445); NMR [$(CD_3)_2SO$] δ 8.77 (t, 1, exchangeable with D_2O, NH), 8.42 (d, 1, J_{AC} = 2 Hz, H_A), 7.80 (dd, 1, J_{BC} = 9 Hz, J_{AB} = 2 Hz, H_C), 7.65 and 7.33 (bd s, 2, exchangeable with D_2O, AsO_3H_2), 7.00 (d, 1, J_{BC} = 9 Hz, H_B), and 4.04 (d, 2,

† From the Department of Biochemistry, the Graduate Program in Physical and Organic Chemistry, and the Scientific Computing Center, State University of New York, Downstate Medical Center, Brooklyn, New York 11203. *Received July 21, 1980; revised manuscript received March 30, 1981.* This work was supported by National Science Foundation Grant PCM 76-21978.

[1] Abbreviations used: RNase A, bovine pancreatic ribonuclease A; DNP, 2,4-dinitrophenyl; 3′-CMP, 3′-cytidylic acid; ANP, 4-arsono-2-nitrophenyl; ANFB, 4-arsono-2-nitrofluorobenzene; CM, carboxymethyl; SNP, 4-sulfono-2-nitrophenyl; Gdn·HCl, guanidine hydrochloride; SNFB, 4-sulfono-2-nitrofluorobenzene; Im, imidazole; DEAE, diethylaminoethyl.

0006-2960/81/0420-4843$01.25/0

J = 5 Hz, α-CH_2). Anal. Calcd for $C_8H_{10}N_3O_6As$: C, 30.11; H, 3.16; N, 13.17; As, 23.48. Found: C, 30.12; H, 3.06; N, 13.07; As, 23.37.

(*B*) *ANP-L-arginine.* ANFB (2.65 g, 10 mmol) and L-arginine hydrochloride (2.1 g, 10 mmol) were dissolved in 65 mL of 1 M triethylammonium bicarbonate, pH 8.0. After 115 h at 50 °C, the solvent was evaporated and the residue codistilled with MeOH. The solid residue was dissolved in water, titrated to pH 3.7 with glacial acetic acid, and cooled to 4 °C. The resulting crystals were collected by filtration and dried to yield 3.09 g (74%). The product was recrystallized 3 times from hot water: vis_{max} (0.2 M sodium phosphate, pH 6) 424 nm (ϵ 5480), vis_{min} 324 nm (ϵ 350); NMR (D_2O + 4 equiv of NaOD) δ 8.28 (d, 1, J_{AC} = 2 Hz, H_A), 7.94 (dd, 1, J_{AC} = 2 Hz, J_{BC} = 9 Hz, H_C), 6.78 (d, 1, J_{BC} = 9 Hz, H_B), 4.04 (t, 1, α-CH), 2.94 (m, 2, δ-CH_2), and 1.70 (m, 4, β- and γ-CH_2). Anal. Calcd for $C_{12}H_{18}N_5O_7As$: C, 34.38; H, 4.33; N, 16.71; As, 17.87. Found: C, 34.48; H, 4.36; N, 16.62; As, 17.82.

(*C*) *ANP-L-argininamide.* ANFB (0.665 g, 2.5 mmol) and L-argininamide dihydrochloride (0.615 g, 2.5 mmol) were mixed in 10 mL of water and titrated to pH 9.6 with 1 M LiOH. The solution was heated in a boiling water bath for 15 min, cooled, and retitrated to pH 9.6. The heating and cooling steps were repeated, and finally the pH was adjusted to 2. Reaction products (7.5 mmol) at pH 2 were applied to a 19 × 8 cm column of Dowex 50-X8 (200–400 mesh) in 0.2 M pyridine–acetic acid, pH 3.10, at 45 °C. The chromatogram was developed by allowing 4 L of 2.0 M pyridine–acetic acid, pH 5.0, to flow into an open mixing vessel initially charged with 4 L of 0.2 M pyridine–acetic acid, pH 3.10. The last of three major fractions, eluting near the mid region of the gradient, was pooled and concentrated to give an orange solid. The residue was dried over P_2O_5 and NaOH to remove pyridine and acetic acid and crystallized from hot water to give 990 mg (32%) of product: vis_{max} (0.2 M sodium phosphate, pH 6) 410 nm (ϵ 4960), vis_{min} 320 nm (ϵ 471); NMR (CF_3COOH) δ 8.92 (s, 1, α-NH), 8.33–7.08 (complex multiplet, 9, H_A, H_B, H_C, amide, guanido NH_2, imino, δ-NH), 6.50 (bd s, 2, AsO_3H_2), 4.60 (m, 1, α-CH), 3.50 (m, 2, δ-CH_2), and 2.25 (m, 4, β- and γ-CH_2). Anal. Calcd for $C_{12}H_{19}N_6O_6As$: C, 34.46; H, 4.58; N, 20.10; As, 17.91. Found: C, 34.44; H, 4.55; N, 20.06; As, 17.90.

(*D*) *α-ANP-L-histidine.* ANFB (0.57 g, 2.15 mmol) and L-histidine (0.156 g, 1 mmol) were mixed in 5 mL of water. The pH was adjusted to 9.5 with 4 N NaOH. After a 5-day period during which 2 equiv of alkali was consumed, L-histidine (0.156 g, 1 mmol) was added and the pH adjusted to and maintained at 9.5 for 48 h. The reaction mixture was brought to pH 8.0, diluted with water to 20 mL, and chromatographed on a 39 × 3.75 cm column of DEAE-cellulose HCO_3^-. The desired compound was eluted by allowing 2 L of 1 M triethylammonium bicarbonate to discharge into an open mixing chamber initially containing 2 L of water. Fractions containing the major peak were pooled and evaporated to a solid. After three codistillations with MeOH, the residue was dissolved in 10 mL of MeOH, and a 6-fold excess of 1 M NaI in acetone was added to precipitate the sodium salt of α-ANP-L-histidine. An additional 100 mL of acetone was added to complete precipitation. The hygroscopic salt was dissolved in a small volume of water and passed 3 times over a column of Dowex 50-X8 (Na form) using water as eluent. The effluent was lyophilized to give 287 mg (30%) of the pure disodium sesquihydrate of α-ANP-L-histidine: vis_{max} (0.2 M sodium phosphate, pH 6) 420 nm (ϵ 5840), vis_{min} 324 nm (ϵ 481); NMR (D_2O) δ 8.30 (s, 2, H_A and C-2), 7.68 (d, 1, J_{BC} = 9 Hz, H_C), 4.47 (s, 1, C-4), 6.85 (d, 1, J_{BC} = 9 Hz, H_B), 4.42 (m, 1, α-CH), and 3.28 (m, 2, β-CH_2). Anal. Calcd for $C_{12}H_{14}N_4O_{8.5}AsNa_2$: C, 30.59; H, 3.00; N, 11.89; As, 15.90. Found: C, 30.49; H, 3.12; N, 11.95; As, 15.71. The product chromatographed as a single peak on the long column of the amino acid analyzer, eluting just after the pH 4.28 buffer change. The absence of 570-nm ninhydrin color indicates the presence of only an α-substituted histidine derivative. Between pH 5.1 and 10.25, 2.12 equiv of alkali was consumed. Since one of these titratable protons must have come from the imidazole group and since the pK_a' of the imidazole ring of Im-DNP-histidine is 3.1 (Henkart, 1971), potentiometric titration supports the presence of only α-ANP-L-histidine.

Other Reagents. α-ANP-L-lysine was obtained from the reaction of ANFB with L-lysine methyl ester at pH 8 (unpublished experiments). ϵ-ANP-L-lysine was prepared by reacting ANFB with the Cu complex of L-lysine at pH 11 (unpublished experiments). 3′-Cytidylic acid was prepared from a mixture of 2′- and 3′-cytidylic acid by a published procedure (Ettinger & Hirs, 1968). ANFB was prepared from the nitration of 4-fluorophenylarsonic acid in HNO_3–H_2SO_4 mixtures (unpublished experiments). All other reagents were obtained commercially and were of the highest purity obtainable.

Protein Concentration. Protein concentration was determined by the method of Lowry et al. (1951) using RNase A as a standard. The extinction coefficient of protein derivatives at 780 nm is unaffected by the ANP group.

Spectrophotometry. Visible absorption spectra (300–600 nm) of ANP derivatives were obtained in 1-cm cells in a Cary Model 14 spectrophotometer at pH 1 in 0.1 M HCl, at pH 6 in 0.2 M sodium phosphate buffer, and at pH 10 in 0.05 M sodium bicarbonate buffer. pH–Difference spectra were observed at 25 °C for solutions of ANP derivatives between pH 1 and 6, 1 and 10, and 6 and 10. In all cases the sample at lower pH was placed in the reference compartment and that at higher pH in the sample compartment.

Spectrophotometric Titration of ANP Derivatives. Spectrophotometric titrations were performed by using a Gilford modified DU-2 spectrophotometer with a Radiometer Model PHM 26 pH meter and titration assembly. ANP derivatives were dissolved in 0.13 M NaCl to give absorbances of approximately 1.0–2.0 at pH 10 in the wavelength range of 445–470 nm. Titrations were carried out in a jacketed reaction cell on 3–5 mL of solution brought to a pH near 10 with 4 N NaOH. Solutions were stirred magnetically and blanketed with a water-saturated stream of N_2. Titrations were performed by using 0.44 N HCl in 0.13 M NaCl delivered manually from a Type SBU1a syringe burette (Radiometer). Sufficient acid was added to reduce the pH of the solution by 0.1–0.15 unit, the solution was transferred to a thermostated 1-cm cuvette, and its absorbance was measured. Duplicate measurements of the pH and the absorbance were made and the values averaged. Transfers between the titration vessel and cuvette were effected through a short piece of 1-mm i.d. Teflon tubing adapted to a Gilson transferator assembly fitted with a 10-cm^3 plastic syringe. Generally, between pH 1.5 and 10.5, 80–90 measurements of the pH and absorbance were made. Absorbance values were corrected for the volume change due to addition of titrant, and a linear correction was applied for base line drift when necessary. The electrode system was calibrated with three standard buffers before and after each experiment. If the discrepancy exceeded 0.05 pH unit, the experiment was discarded. Temperatures in the cuvette and titration vessel were maintained individually to

within 0.05 °C and agreed with each other to within 0.1 °C. CO_2-Free water was used to prepare all solutions for titration.

Absorbance–pH data for α-ANP-L-argininamide, ε-ANP-L-lysine, ANFB, ANP glycinamide, 41-SNP RNase A, 1-α-ANP RNase A, performic acid oxidized 41-ANP RNase A, 41-ANP RNase A in 6 M Gdn·HCl, *N*-3-CM-His-12 41-ANP RNase A, and *N*-1-CM-His-119 41-ANP RNase A were fitted to

$$\frac{A}{C_t} = \frac{\alpha(H)^2 + \beta(H) + \gamma}{\delta(H)^2 + \mu(H) + \lambda} \quad (1)$$

derived from the ionization model

$$RAsO_3H_2 \overset{K_1}{\rightleftharpoons} RAsO_3H^- \overset{K_2}{\rightleftharpoons} RAsO_3^{2-} \quad (2)$$

where α is $\epsilon_m(RAsO_3H_2)$, β is $\epsilon_m(RAsO_3H^-)K_1$, γ is $\epsilon_m(RAsO_3^{2-})K_1K_2$, δ is 1, μ is K_1, and λ is K_1K_2. A is the absorbance, (H), the hydrogen ion concentration, and C_t, the total concentration of the ANP derivative. For the low-pH regions of the titration curves of α-ANP-L-lysine and α-ANP-L-arginine, and the first and second inflections of the α-ANP-L-histidine curve, as well as the low- and high-pH regions of the 41-ANP RNase A and 41-ANP RNase A plus uridine titrations, absorbance–pH data were fitted to eq 1, derived from the model of Shrager et al. (1972) for the ionization of a prototropic species in the presence of a single interacting group. For the first inflection of α-ANP amino acids, this model is

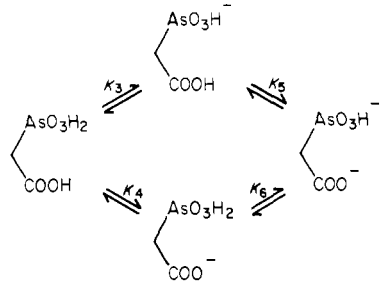

(3)

where α is $\epsilon_m(AsO_3H_2, COOH)$, $\beta = \epsilon_m(AsO_3H^-, COOH)K_3 + \epsilon_m(AsO_3H_2, COO^-)K_4$, $\gamma = \epsilon_m(AsO_3^-, COO^-)K_3K_5$, $\delta = 1$, $\mu = K_3 + K_4$, and $\lambda = K_3K_5$. Also, $K_3K_5 = K_4K_6$. Models of similar forms were utilized to analyze the data from the second α-ANP-L-histidine inflection as well as these from the 41-ANP RNase A titrations. Spectrophotometric titration data were fitted to the appropriate equation by using the BMDPAR-Derivative-Free Nonlinear Regression from Ralston (1977).

3′-CMP Binding Experiment. To 4 mL of 3×10^{-4} M 41-ANP RNase A in 0.1 M sodium acetate buffer, pH 5.5, 0.47 mL of 0.2 M 3′-CMP in the same buffer was added in small increments at 25 °C. After each addition the solution was transferred to a 1-cm cuvette and the absorbance at 450 nm was recorded. Forty measurements were made as the 3′-CMP varied up to 0.0208 M. Corrections were made for the decrease in absorbance and protein concentration upon dilution. The data for the binding of 3′-CMP to 41-ANP RNase A were fitted to

$$K = \frac{\Delta A/\Delta\epsilon}{(E_0 - \Delta A/\Delta\epsilon)(L_0 - \Delta A/\Delta\epsilon)} \quad (4)$$

described by Hammes & Schimmel (1965) in which E_0 and L_0 are the total concentrations of 41-ANP RNase A and 3′-CMP, respectively, and ΔA is the increase in absorbance accompanying ligand binding. Values of K, the association constant for 1:1 complex formation, and $\Delta\epsilon$, the extinction difference between liganded and unliganded 41-ANP RNase A, were estimated from a nonlinear regression analysis using the BMDPAR program cited above.

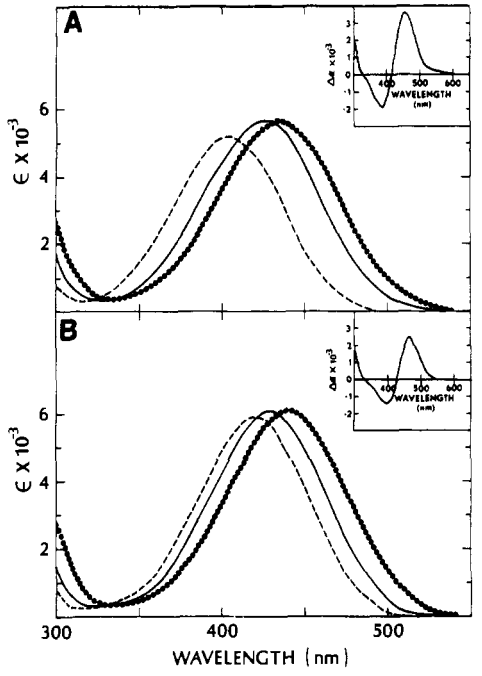

FIGURE 1: Absorption spectra of α-ANP-L-lysine (A) and ε-ANP-L-lysine (B) at pH 1 (---) (0.1 M HCl), pH 6 (—) (0.2 M sodium phosphate), and pH 10 (●) (0.05 M sodium bicarbonate).

Results and Discussion

Spectrophotometry of Model Compounds. Figure 1 depicts the effect of pH on the absorption properties of α- and ε-ANP-L-lysine. The pH values selected ensure that only one prototropic form of the dibasic aromatic arsonic acid is represented by the spectrum. With successive proton dissociations, red shifts occur in the wavelength of maximum absorption while the extinction coefficients remain essentially constant. The shifts in the absorption maxima with pH produce difference spectra in which $\Delta\epsilon_{max}$, the difference extinction coefficient at the wavelength of maximum difference, is 50% or more of the extinction coefficient of either component at their respective maximum (cf. Figure 1, inset).

Table I lists the spectral properties of various ANP amino acids including derivatives of L-lysine in which the effect of α or ε substitution may be compared. Derivatives of glycinamide and L-argininamide exhibit bathochromic spectral shifts similar in magnitude between pH 1 and 6 as well as between pH 6 and 10. However, for α-substituted derivatives which possess an α-carboxyl group $\Delta\lambda$ for pH 1–6 exceeds $\Delta\lambda$ for pH 6–10 by a factor of 2.

Spectrophotometric Titration of Model Compounds. Large spectrophotometric changes accompanying successive deprotonation of nitrophenylarsonic acids prompted us to use this property to determine ionization constants of ANP amino acid derivatives. Figure 2A shows changes in the absorbance at 466 and 477 nm during the titration of ε-ANP-L-lysine in dilute NaCl and 6 M Gdn·HCl solutions, respectively. For this compound as well as α-ANP amino acid amides (cf. Table II and Figure 2B, curve 2), $\Delta\epsilon$ for each ionization is essentially similar for each dissociation. Also, $\Delta\epsilon_{max}$ is temperature independent between 10 and 70 °C.

Figure 2B (curve 1) reveals that α-ANP-L-arginine has a much greater change in $\Delta\epsilon$ at 455 nm between pH 1 and 6 than between pH 6 and 10 due to the α-carboxyl group ionization. In contrast, carboxyl group ionization does not perturb the spectrophotometric response of ε-ANP-L-lysine in the acidic region, similar to that observed for α-ANP-L-argininamide and ANP glycinamide. Similar effects exist in the titration of DNP

Table I: Visible Spectral Data for ANP Amino Acid Derivatives[a]

compound	pH	λ_{max} (nm)	ϵ_{max} (M^{-1} cm^{-1})	λ_{min} (nm)	ϵ_{min} (M^{-1} cm^{-1})	pH 1/pH 10 $\Delta\lambda_{max}$ (nm)	pH 1/pH 10 $\Delta\epsilon_{max}$ (M^{-1} cm^{-1})	pH 1/pH 6 $\Delta\lambda_{max}$ (nm)	pH 1/pH 6 $\Delta\epsilon_{max}$ (M^{-1} cm^{-1})	pH 6/pH 10 $\Delta\lambda_{max}$ (nm)	pH 6/pH 10 $\Delta\epsilon_{max}$ (M^{-1} cm^{-1})
α-ANP-lysine	1	405	5420	314	336	455	3140	448	2770	468	1330
	6	426	5670	323	346						
	10	435	5650	330	432						
ε-ANP-lysine	1	420	5880	317	292	467	2410	460	1240	473	1300
	6	427	6070	325	249						
	10	440	6080	335	359						
ANP-arginine	1	403	5030	314	359	455	3210	477	2370	465	1100
	6	424	5480	324	350						
	10	434	5470	327	405						
ANP-argininamide	1	403	4990	314	375	446	1740				
	6	410	4960	320	471						
	10	418	5010	327	586						
ANP-glycinamide	1	403	5580	314	390	445	1800	438	950	450	920
	6	410	5620	318	445						
	10	415	5520	325	557						
α-ANP-histidine	1	400	5320	315	446	454	3610	444	2380	465	1540
	6	420	5840	324	481						
	10	434	5850	333	531						
ANFB	1	248	3390	228	2320	267	2140				
	10	246	3290	233	2130						

[a] All spectra were obtained at 25 °C on a Cary Model 14 UV-vis spectrophotometer. Solvent conditions at pH 1, 6, and 10 were as described in Figure 1.

Table II: Spectrophotometer Titration of ANP Amino Acid Derivatives

compound	λ (nm)	concn (M × 10^4)	pK_1'	pK_2'	ε ($RAsO_3H_2$) (M^{-1} cm^{-1})	ε ($RAsO_3H^-$) (M^{-1} cm^{-1})	ε ($RAsO_3^{2-}$) (M^{-1} cm^{-1})
ANFB							
5 °C	267	2.18	2.31	7.35	3300	4635	5790
35 °C	267	2.60	2.50	7.30	3704	4890	6092
α-ANP-argininamide							
10 °C	446	2.96	3.03	8.05	1860	2620	3510
25 °C	446	3.19	3.08	7.90	1860	2640	3530
40 °C	446	4.25	3.12	7.79	1880	2650	3480
55 °C	446	3.83	3.16	7.86	1960	2730	3540
70 °C	446	3.83	3.12	7.82	1810	2410	3210
α-ANP-arginine							
25 °C	455	3.98	*a*	7.98	*a*	3530	4420
40 °C	455	3.98	*a*	7.96	*a*	3610	4520
ANP-glycinamide, 25 °C	445	3.30	3.24	8.22	2090	2970	3940
ANP-glycinamide, 6 M Gdn·HCl, 25 °C	455	6.34	2.96[b]	6.99[b]	2770	3550	4180
α-ANP-lysine, 25 °C	453	4.08	*a*	8.09	*a*	3920	4810
ε-ANP-lysine							
10 °C	466	3.31	3.27	8.24	2150	3260	4460
25 °C	466	3.31	3.25	8.15	2180	3290	4550
40 °C	466	3.31	3.38	8.11	2170	3240	4390
55 °C	466	3.31	3.37	8.09	2340	3390	4500
70 °C	466	3.68	3.51	8.06	2430	3540	4710
ε-ANP-lysine, 6 M Gdn·HCl, 25 °C	477	2.87	3.02[b]	7.25[b]	1450	2350	3470

[a] Cf. Table III. [b] pK_a' values are apparent values uncorrected for the effect of Gdn·HCl on the electrode response and water activity.

amino acids (Ramachandran & Sastry, 1962). Figure 2A (curve 1) also indicates that there are no spectral perturbations associated with ionization of the α-amino group of ε-ANP-L-lysine since the region between pH 9 and 11 is relatively flat. Titration of ε-ANP-L-lysine to pH 0 produces no further spectrophotometric changes which result from protonation of the compound in strong acid.

The spectrophotometric titration of the α-ANP-L-histidine derivative is influenced by the titration of the imidazole group (cf. Table III). $\Delta\lambda_{max}$ between pH 6 and 10 is 14 nm compared to 9–10 nm for other α-ANP amino acids (cf. Table I). Also, $\Delta\epsilon_{max}$ for α-ANP-L-histidine between pH 6 and pH 10 is substantially greater than $\Delta\epsilon_{max}$ for other α-ANP amino acid derivatives.

Titration data for α-ANP amino acids in the low-pH region were fitted to eq 1 derived from the ionization model given by eq 3. The high-pH inflection of α-ANP-L-histidine was analyzed according to the model

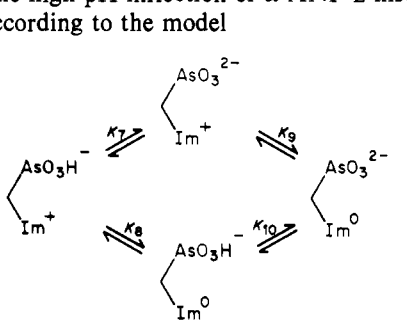

(5)

and eq 1 in which α is $\epsilon_m(AsO_3H^-, Im^+)$, β = $\epsilon_m(AsO_3^{2-},$

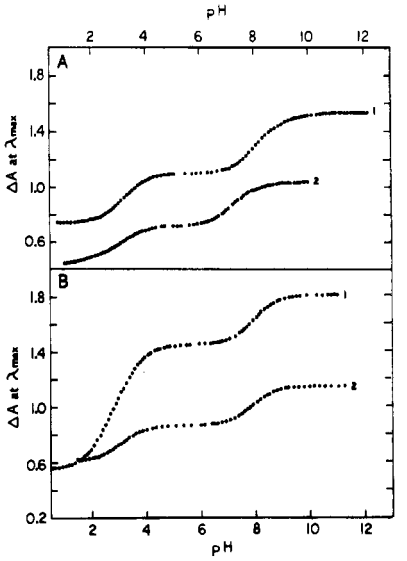

FIGURE 2: Spectrophotometric titration of representative ANP amino acid derivatives: (A) (curve 1) 3.31×10^{-4} M ϵ-ANP-L-lysine, λ = 466 nm, 25 °C; (curve 2) 2.87×10^{-4} ϵ-ANP-L-lysine in 6 M Gdn·HCl, λ = 477 nm, 25 °C; (B) (curve 1) 3.98×10^{-4} M α-ANP-L-arginine, λ = 455 nm, 25 °C; (curve 2) 3.19×10^{-4} M α-ANP-L-argininamide, λ = 466 nm, 25 °C. The solvent was 0.13 M NaCl.

$Im^+)K_7 + \epsilon_m(AsO_3H^-, Im^0)K_8$, $\gamma = \epsilon_m(AsO_3^{2-}, Im^0)K_7K_9$, $\delta = 1$, $\mu = K_7 + K_8$, and $\lambda = K_7K_9$.

For eq 3 and 5, there are four independent extinction coefficients and three independent microscopic ionization constants which determine the values of the five independent coefficients of eq 1. Only values of $\epsilon_m(AsO_3H_2, COOH)$ and $\epsilon_m(AsO_3^{2-}, COO^-)$ for α-ANP amino acids and $\epsilon_m(AsO_3H^-, Im^+)$ and $\epsilon_m(AsO_3^{2-}, Im^0)$ for α-ANP-L-histidine may be uniquely determined (Shrager et al., 1972). None of the microscopic dissociation constants can be computed. This problem was resolved by assuming values for K_3' and K_7' based on titrations of model compounds. It is assumed that the –COOH and the $-CONH_2$ groups are electronically and sterically very similar such that the K_3' microscopic dissociation constant for α-ANP-L-arginine, α-ANP-L-lysine, and α-ANP-L-histidine is identical with the macroscopic constant observed for α-ANP-L-argininamide. This permits the evaluation of K_4', K_5', and K_6' of eq 3 for all the α-ANP amino acids (cf. Table IV). Also, it is assumed that the second macroscopic ionization constant for α-ANP-L-arginine and α-ANP-L-lysine accurately predicts the value of the microscopic constant, K_7', for the second α-ANP-L-histidine inflection. No attempt has been made to evaluate the extinction coefficients of the intermediate forms in eq 3 and 5.

Temperature Dependence. For ANFB, pK_1' is 2.31 at 5 °C and increases by 0.2 pH unit at 35 °C. The second dissociation of ANFB at 5 °C is characterized by a pK_2' value of 7.35 which falls to 7.30 at 35 °C (cf. Table II). These results are consistent with the known behavior of H_3AsO_4 (Izatt & Christensen, 1968) in which the first dissociation is accompanied by a negative enthalpy and the second by a positive enthalpy of ionization.

pK_1' and pK_2' values were determined for ϵ-ANP-L-lysine and α-ANP-L-argininamide from 10 to 70 °C at 15 °C intervals. The temperature dependence was assumed to obey the van't Hoff law, and values for the enthalpy of ionization calculated for ϵ-ANP-L-lysine for the first and second arsonate dissociations are −1.7 ± 0.97 and 1.3 ± 0.34 kcal/mol, respectively. For α-ANP-L-argininamide, corresponding values for the first and second ionizations are −1.28 ± 0.10 (excluding

Table III: Microscopic Dissociation Constants and Extinction Coefficients for α-ANP Amino Acids and ANP Protein Derivatives Fitted to Equations 1, 3, and 5

compound	λ (nm)	concn ($M \times 10^6$)	pH range	ϵ_{max} (H_2O_3As, COOH) (M^{-1} cm^{-1})	ϵ_{max} ($^-HO_3As$, COO^-) (M^{-1} cm^{-1})	pK_3'	pK_6'	pK_4'	pK_5'	pK_7'	pK_{10}'	pK_8'	pK_9'
α-ANP-lysine, 25 °C	453	4.08	acid	1530	3920	3.08	3.35	2.67	2.92				
α-ANP-histidine, 25 °C	455	2.30	acid	1200	3270	3.08	3.31	2.29	2.51				
			alkaline	3250[a]	4680[a]					8.03	8.17	6.89	7.03
α-ANP-arginine 25 °C	455	3.98	acid	1620	4070	3.08	3.33	2.67	2.92				
40 °C	455	3.98	acid	1140	3610	3.12	3.34	2.54	2.76				
41-ANP RNase A, 25 °C	468	*d*	4.1–9.4	2100[b]	3980[b]					5.86 ± 0.02[e]	7.01 ± 0.04[e]	6.79	7.95 ± 0.02[e]
41-ANP RNase A, 25 °C	468	*d*	1.0–4.3	1790[c]	2130[c]	1.40[f]	3.14[f]	1.88[f]	3.62				

[a] Extinction coefficients refer to the following ionization states: 3250, $^-HO_3As(COO^-)Im^+$; 4680, $^{2-}O_3As(COO^-)Im$. [b] Extinction coefficients refer to the following ionization states: 1790, $H_2O_3As(COOH)Im^+$; 2130, $^-HO_3As(COO^-)Im^+$. [d] The protein concentration ranged from 2.1×10^{-4} to 3.04×10^{-4} M. [e] pK_a' values represent the mean and standard deviation of four titration experiments. The residual sum of squares ranged from 2.57×10^{-4} to 6.12×10^{-4}. [f] pK_a' values represent the mean of two titration experiments. The standard deviations for the estimates of pK_3', pK_6', and pK_4' are all 0.01 pH unit. The residual sum of squares ranged from 1.26×10^{-5} to 1.32×10^{-5}.

Table IV: Spectrophotometric Titration of ANP Protein Derivatives Fitted to Equations 1 and 2

compound	λ (nm)	concn ($M \times 10^4$)	pH range	pK_1'	pK_2'	ϵ ($RAsO_3H_2$) (M^{-1} cm^{-1})	ϵ ($RAsO_3H^-$) (M^{-1} cm^{-1})	ϵ ($RAsO_3^{2-}$) (M^{-1} cm^{-1})
41-ANP RNase A, 70 °C	468	3.04	1.5–4.1	2.99	[a]	1760	2530	[a]
41-SNP RNase A, 25 °C	475	1.02	2.7–8.6	3.62	6.79	11600[b]	10780[b]	11800[b]
41-ANP RNase A, 6 M Gdn·HCl, 25 °C	468	3.04	1.2–8.7[c]	3.11[d]	7.34[d]	1560	2230	2840
performic acid oxidized 41-ANP RNase, A 25 °C	468	3.38	1.9–9.6	3.15	8.12	1050[e]	1580[e]	2100[e]
41-ANP RNase A + 3′-CMP, 25 °C	468	2.43	3.4[f]–9.4	4.86	8.03	2526	3000	3890
CM-His-12 41-ANP RNase A, 25 °C	468	2.29	0.83–9.5	2.24	6.99	1543	2230	2930
CM-His-119 41-ANP RNase A, 25 °C	468	2.57	1.1–9.3	2.59	7.60	2140	3070	4450
1-α-ANP RNase A, 25 °C	449	1.04	1.6–9.5	3.18	7.76	2600	3590	4900
1-α-ANP RNase A + 3′-CMP, 25 °C	449	1.04	1.5–10.3	3.20	7.85	2740	3860	5330

[a] Additional titration parameters could not be determined due to irreversible effects above pH 4.1. [b] Extinction coefficients refer to the following ionization states of the protein: 11 600, $^-O_3S(Im^+)COOH$; 10 780, $^-O_3S(Im^+)COO^-$; 11 800, $^-O_3S(Im)COO^-$. [c] Recorded pH values are the observed values and are uncorrected for the effects of Gdn·HCl. [d] pK_a' values are apparent values uncorrected for the effect of Gdn·HCl on the electrode response. [e] Values may be low due to partial destruction during performic acid oxidation. [f] Measurements below pH 3.4 could not be made due to precipitation of 3′-CMP.

the 70 °C value) and 1.55 ± 1.3 kcal/mol. These values compare favorably with the ionization enthalpies of the first and second dissociations for H_3AsO_4 which are −1.69 and 0.77 kcal/mol, respectively (Izatt & Christensen, 1968). Large errors in the thermodynamic parameters are related to the low absolute values of the ionization enthalpies. The insensitivity of the arsonic acid dissociations to temperature is important if the ANP reporter group is to be a useful microenvironmental probe of the thermal denaturation of proteins. At a pH where the reporter group is undergoing ionization, the total absorbance change will be a function of the change in the microenvironment of the probe as increasing temperature produces conformational unfolding in its vicinity plus the variation in the ratio of acidic to basic forms of the partially ionized probe. The ionization enthalpies for the ANP group are very small, indicating that the contributions of changing pK_a' values with varying temperature will make small or negligible contributions to the overall absorbance change as the protein passes through the thermal transition.

Spectrophotometric Titration of Protein Derivatives. (A) 41-ANP RNase A. The spectrophotometric titration of 41-ANP RNase A is depicted in Figure 3. At 25 °C the titration is fully reversible between pH 0.65 and pH 10.85. Incubation of 41-ANP RNase A at either pH extreme for 1 h does not affect the titration curve. For interpretation of the spectral changes, the curve was divided into three regions: an acidic region extending from pH 1 to pH 4.3, a neutral region ranging from pH 4.3 to pH 9.0, and an alkaline segment above pH 9.0.

Two separate inflections near pH 6 and pH 8 are observed in the neutral region. No distinctive inflection appears around pH 3 which would normally be associated with the first dissociation of the arsonic acid group. Studies with the model compound, 41-SNP RNase A (cf. Table IV and Figure 3), rule out the possibility that the first dissociation is shifted 3 pH units to account for the appearance of the new inflection at pH 6. The active site possesses anion binding capability (Wyckoff et al., 1970). An excess of positive charge would stabilize the anionic form of the ANP group and give rise to an environment in which the ANP moiety behaves as a stronger and not a weaker acid. An increase in pK of 3 pH units would require that the ANP group be free from the electrical influence of the active site and be forced into a region of high negative potential. Evidently, this is not the case.

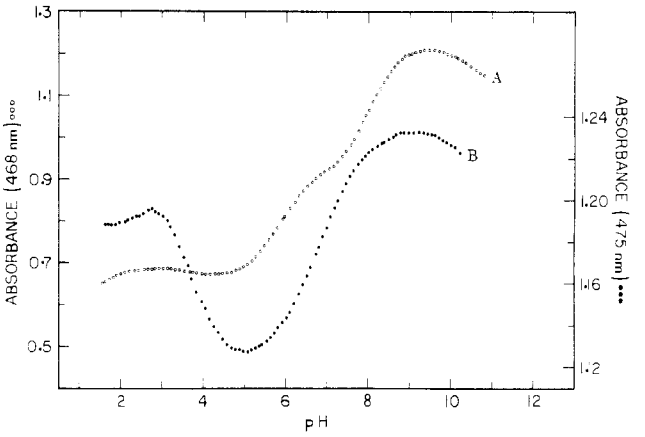

FIGURE 3: Spectrophotometric titration of 41-ANP RNase A, 3.04 × 10^{-4} M, λ = 468 nm, 25 °C (A), and 41-SNP RNase A, 1.02 × 10^{-4} M, λ = 475 nm, 25 °C (B). The solvent was 0.13 M NaCl.

Between pH 1 and 14 the SNP moiety possesses no ionizable groups, yet the titration curve of 41-SNP RNase A has two inflections, one centered at pH 3.62 and a second at pH 6.79. The latter inflection is most probably associated with the ionizations of one or both of the active-site histidine residues that have been shown by NMR titration to possess pK_a' values of 5.8 (His-12) and 6.2 (His-119) in the native enzyme (Patel et al., 1975). The pK_a' values of His-12 and His-119 rise to over 8 in the presence of saturating concentrations of either 2′- or 3′-CMP (Meadows et al., 1969). The average pK_a' increase of 0.8 pH unit for His-12 and His-119 in 41-SNP RNase A relative to the native enzyme indicates the existence of a relatively strong interaction between the SNP anion and the positively charged imidazolium ions. The SNP and ANP groups are essentially isosteric, and it is expected that the arsonate moiety would bind in the same region as the sulfonate ion. Because the arsonate group is dianionic, a much stronger interaction with the active-site histidine residues is possible. This interpretation would assign the inflection centered on pH 8.0 to the titration of both active-site histidine residues. The strong charge–charge interaction would be in harmony with the sizeable reduction in pK_a' of the active-site-bound ANP group from 8.1 to 5.8. This is consistent with the reduction in pK_a' from 6.1 to 4.4 for the dissociation of the monobasic phosphate of 3′-CMP in the 3′-CMP–RNase A complex

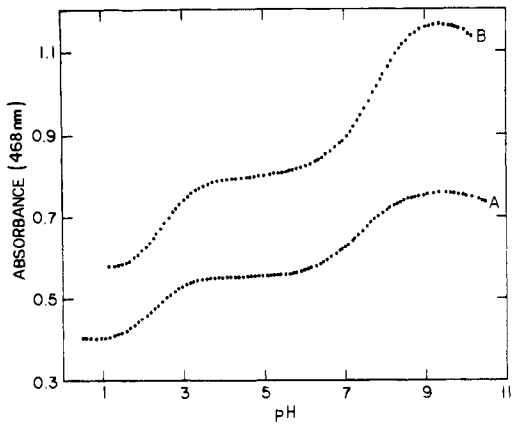

FIGURE 4: Spectrophotometric titration of carboxymethyl derivatives of 41-ANP RNase A: (A) *N*-3-CM-His-12 41-ANP RNase A, 2.29 × 10^{-4} M, λ = 468 nm, 25 °C; (B) *N*-1-CM-His-119 41-ANP RNase A, 2.57 × 10^{-4} M, λ = 468 nm, 25 °C. Both titrations were carried out in 0.13 M NaCl.

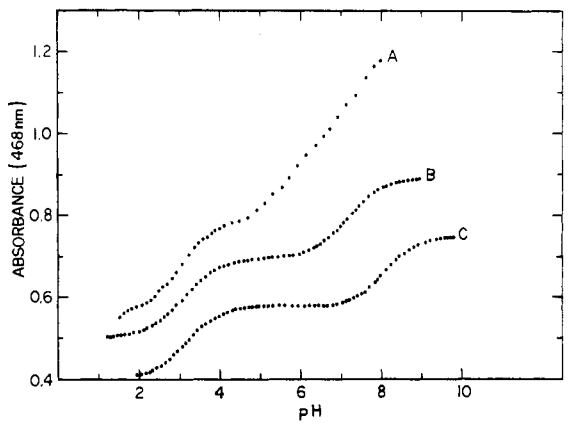

FIGURE 5: Spectrophotometric titration of 41-ANP RNase A under denaturing conditions: (A) 41-ANP RNase A, 3.04 × 10^{-4} M, λ = 468 nm, 70 °C; (B) 41-ANP RNase A in 6 M Gdn·HCl, 3.04 × 10^{-4} M, λ = 468 nm, 25 °C; (C) performic acid oxidized 41-ANP RNase A, 3.38 × 10^{-4} M, λ = 468 nm, 25 °C. The solvent was 0.13 M NaCl.

(Gorenstein & Wyrwicz, 1973). Further support comes from an analysis of the titration curves for *N*-3-CM-His-12 41-ANP RNase A and *N*-1-CM-His-119 41-ANP RNase A (cf. Table IV and Figure 4). . After introduction of an additional negative center, the second arsonate ionization is not completely normalized in either derivative. The lower pK_a' values for $RAsO_3H^-$ ionization compared with performic acid oxidized 41-ANP RNase A indicate the preservation of substantial electrostatic interaction between the ANP group and the positive center after carboxymethylation.

An inflection near pH 3, normally associated with the first dissociation of the arsonic acid group, is absent. However, when 41-ANP RNase A is titrated at 70 °C, a temperature above the T_m for the thermal transition, an inflection centered near pH 3.0 is found (cf. Table IV and Figure 5, curve A). This inflection suggests that raising the temperature produces an expulsion of the ANP group from the active site with normalization of its ionization properties. Data for the determination of pK_a' at 70 °C were obtained below pH 4.0 because of irreversible effects above this pH (Tsong et al., 1970). Furthermore, the titration curve of 41-SNP RNase A indicates a second inflection in the acidic region centered at pH 3.62. This change, unrelated to SNP group ionization, probably reflects the acid-promoted destruction of the active site with conformational reorientation of the SNP group. Such an effect may be associated with protonation of Asp-121 which is thought to stabilize the positive charges at the active site.

The uncharacteristic behavior of 41-ANP RNase A in the acidic range may reside in the superposition of two titration effects. As the pH is decreased protonation of an active-site carboxylate anion and the monobasic arsonate occurs simultaneously producing opposing absorbance changes. Therefore, attempts were made to fit the data for the titration of 41-ANP RNase A between pH 1.0 and 4.3 to the model depicted by eq 3. The coefficients of the nonlinear regression fitted to eq 1 may be constrained by assigning values of either K_3' or K_5' based on titrating 41-ANP RNase A at 70 °C or 41-SNP RNase A at 25 °C, respectively. The latter is a more reasonable choice because the conformations of 41-ANP and 41-SNP RNase A are probably identical in this pH range, whereas the conformations at 25 °C and 70 °C may be substantially different. The value of pK_5' for the carboxylic acid dissociation in the presence of a fixed monoanionic charge was assumed to be identical with the pK_a' for the acid inflection in the 41-SNP RNase A titration (cf. Table III). Reduction of pK_3' by over 1.5 pH units suggests that in 41-ANP RNase A the positively charged cluster(s) which form the anion-binding region may survive in relatively strong acid. The normalization of pK_3' following dissociation of Asp-121 suggests that the carboxylate anion plays a significant role in stabilizing the anion-binding site. Since concurrent deprotonation of carboxyl groups in α-ANP amino acids is associated with an increase in the extinction (cf. Figure 2B), the opposite effect in the 41-ANP RNase A titration implies that ionization of Asp-121 causes a local movement of the ANP moiety to a new environment.

The alkaline limb of the titration curve was not analyzed in detail because of the likelihood of irreversible denaturation at pH values above 11. Above pH 9.5 the absorbance decreases in the 41-ANP and 41-SNP RNase A titrations (cf. Figure 3) while it remains pH independent for the ε-ANP-L-lysine curve (cf. Figure 2) and for 41-ANP RNase A denatured either by performic acid oxidation or by solution in 6 M Gdn·HCl (cf. Figure 5). This suggests that the chromophore in native 41-ANP RNase A is responding further to changes which alter the charge status of the active center. Deprotonation of additional lysine residues, perhaps of Lys-7, could account for the decreasing absorbance in the region of pH 10.

(B) Spectrophotometric Titration of 41-ANP RNase A in the Presence of Active-Site Ligands. The maximum binding affinity of pyrimidine nucleotides for RNase A occurs at pH 5.5 and rapidly falls off on either side of the pH optimum (Anderson et al., 1968). Although 0.1 M 3′-CMP was used during the titration of 41-ANP RNase A, it is doubtful that saturating concentrations of the nucleotide persist above pH 8. Hence, the structural feature associated with the inflection centered on pH 8 (cf. Figure 6, curve A) cannot be interpreted with any certainty. Absorbance changes in this region may arise due to interaction of the ANP group with active-site histidine residues or with 3′-CMP, as well as titration of the ANP group itself. A second inflection centered on pH 4.86 with a reduced value of Δε for the transition of 480 M^{-1} cm^{-1} is probably due to the presence of 3′-CMP. The inflection centered at pH 5.8 is unliganded 41-ANP RNase A and previously attributed to the ionization of monobasic arsonate is absent in the 3′-CMP titration. Binding of the phosphate moiety of 3′-CMP may be expected to displace the arsonate residue from its ionic interactions with the positive centers at the active site. Expulsion of the ANP group would tend to normalize its ionization and result in protonation of the dibasic

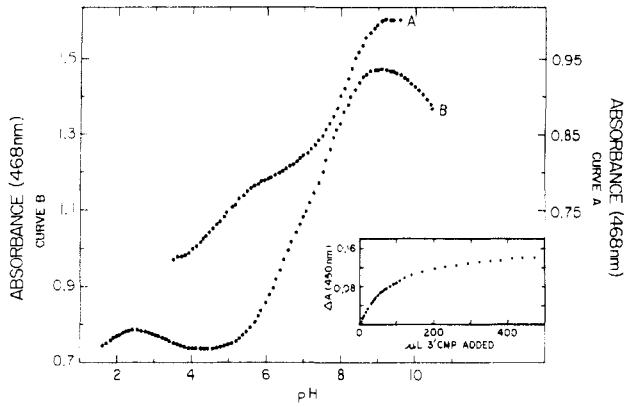

FIGURE 6: Spectrophotometric titration of 41-ANP RNase A in the presence of ligands and the binding of 3′-CMP to 41-ANP RNase A: (A) 41-AMP RNase A plus 0.1 M 3′-CMP, 2.43×10^{-4} M protein, $\lambda = 468$ nm, 25 °C; (B) 41-ANP RNase A plus 0.1 M uridine, 3.49×10^{-4} M protein, $\lambda = 468$ nm, 25 °C. (Inset) The variation of the absorbance at 450 nm upon the serial addition of 3′-CMP to 41-ANP RNase A. The solvent was 0.1 M sodium acetate buffer, pH 5.5. Absorbance values were sampled for 39 different 3′-CMP concentrations. Nonlinear regression fitted to eq 4 gave for the average of two experiments a residual sum of squares of 1.034×10^{-4}.

arsonate ion. Other structural rationalizations are equally plausible. For example, the low-pH inflection could receive contributions from a recognized conformational change in the 3′-CMP–enzyme complex (French & Hammes, 1965) or protonation of an ionized carboxyl group in the 41-ANP RNase A–3′-CMP complex (Cathou & Hammes, 1965). Alternatively, contributions to the absorbance changes could arise from protonation of the phosphate moiety of bound 3′-CMP. It is possible that one or more of the effects cited could influence the inflection at pH 4.86, and it is impossible to assign a major role to any one process.

Uridine binding is pH independent over most of the titration range (Pincus et al., 1975; Ukita et al., 1961; Lindquist et al., 1973). The titration curves for 41-ANP RNase A (cf. Figure 3) and 41-ANP RNase A plus uridine (cf. Figure 6) show small differences in both the acidic and neutral regions. Nucleoside binding raises the pK_a' of His-12 of RNase A from 5.8 to 6.4 (Meadows et al., 1969; Patel et al., 1975). It is expected, therefore, that uridine binding to 41-ANP RNase A would modify the interaction between the arsonate anion and the histidine residues. The extinction coefficients for the predominant species at pH 9.3 are 3980 and 4240 M^{-1} cm^{-1} for the 41-ANP RNase A and 41-ANP RNase A plus uridine curves, respectively. At pH 4.1 ϵ_{max} values are essentially identical, 2100 and 2040 M^{-1} cm^{-1} for the same two titrations. However, at pH 1.0, ϵ_{max} values are significantly different, suggesting that the nucleoside interaction persists in strong acid. Lack of a suitable model and uncertainty as to the extent of saturation throughout the pH range studied have prevented the assignment of pK_a' values.

(C) Spectrophotometric Titration of N-3-CM-His-12 41-ANP RNase A and N-1-CM-His-119 41-ANP RNase A. Alkylation with either 2′(3′)-(*O*-bromoacetyl)uridine or bromoacetate produces carboxymethyl 41-ANP RNase A derivatives in which His-12 and His-119, respectively, are modified (Crestfield et al., 1963; Pincus & Carty, 1970; Pincus et al., 1975). Carboxymethylation may be expected to diminish the interaction of the arsonate dianion with the active-site imidazolium ions, an effect which would tend to normalize the titration of the ANP group. This is evident in Figure 4 in which the usual double inflection observed for the titration of model compounds is seen. However, each curve demonstrates that interactions between the ANP group and positive charges at the active site still persist. First, both curves show a fall in absorbance in the alkaline region, characteristic of the 41-ANP RNase A titration, but not of that of model compounds. Second, both derivatives show unusually low inflections in the acidic and alkaline limbs of the titrations. For *N*-3-CM-His-12 41-ANP RNase A, pK_1' and pK_2' values, interpreted as the first and second ionizations of the ANP group, are 2.24 and 6.99, 0.9 unit and 1.1 pH units below pK_1' and pK_2' for performic acid oxidized 41-ANP RNase A. Similarly, for *N*-1-CM-His-119 41-ANP RNase A, pK_1' and pK_2' values are 0.56 and 0.52 pH unit below those obtained for the denatured RNase A derivative. Carboxymethylation of either active-site histidine apparently induces a relocation of the ANP group to another region of high positive charge which must persist throughout the pH range and is probably associated with nearby lysine and arginine residues. In addition to the positive center associated with His-12 and His-119, more positive charge composed of Lys-7, Arg-10, and Arg-39 is clustered near the active site (Loeb & Saroff, 1964).

Reduction in the values of pK_1' and pK_2' for *N*-3-CM-His-12 41-ANP RNase A is roughly twice as great as that for the His-119 derivative compared to the performic acid oxidized 41-ANP protein. This difference may be due to the greater proximity of the ANP group to the His-119 than to the His-12 side chain in 41-ANP RNase A. Carboxymethylation of His-119 would produce greater disruption of ANP binding resulting in a larger displacement of the chromophore from the active-site region. Carboxymethylation of His-12 may not perturb the ANP moiety as extensively, permitting the arsonate dianion to interact more favorably with the positive center, giving rise to lower values of pK_1' and pK_2' for *N*-3-CM-His-12 41-ANP RNase A. This interpretation is consistent with kinetic data (unpublished experiments) which show that the relative rate of alkylation of 41-ANP RNase A to that of RNase A is much greater for 2′(3′)-(*O*-bromoacetyl)uridine than for bromoacetic acid at pH 5.5.

(D) Denatured Forms of 41-ANP RNase A. The values for pK_1' and pK_2' of 3.15 and 8.12 for performic acid oxidized 41-ANP RNase A (cf. Table IV) compare favorably with those for ϵ-ANP-L-lysine at 25 °C, 3.25 and 8.15, respectively. Similarly, the shape of the curve and apparent pK_a' values for 41-ANP RNase A in 6 M Gdn·HCl are nearly identical with those obtained for ϵ-ANP-L-lysine under similar solvent conditions. Values of pK_1' and pK_2' for the enzyme derivative are 3.11 and 7.34, respectively, while those for ϵ-ANP-L-lysine in 6 M Gdn·HCl are 3.02 and 7.25, respectively. These results suggest that the anomalous curve for 41-ANP RNase A is a result of the stereospecific association of the ANP moiety with residues at the catalytic center of the enzyme and that the titration curve of 41-ANP RNase A is normalized under conditions where the protein is denatured.

(E) 1-α-ANP RNase A. The titrations of 1-α-ANP RNase A and α-ANP-L-argininamide are essentially identical (cf. Figures 2 and 7). pK_a' values for the first and second dissociations of 1-α-ANP RNase A are 3.18 and 7.76 and for the argininamide derivative are 3.08 and 7.90. The pK_a' values obtained for 1-α-ANP RNase A in the presence and absence of 3′-CMP (cf. Table IV) indicate that the ANP moiety attached to the α-amino group is unresponsive to nucleotide binding at the active site. This argues that the N-terminal segment of native RNase A is remote from the active-site cleft.

(F) Binding of 3′-CMP to 41-ANP RNase A. The equilibrium dissociation constant, *K*, of 3′-CMP from its complex with 41-ANP RNase A is 3.78 ± 0.08 mM, 300 times greater than the value for dissociation of the RNase A–3′-CMP

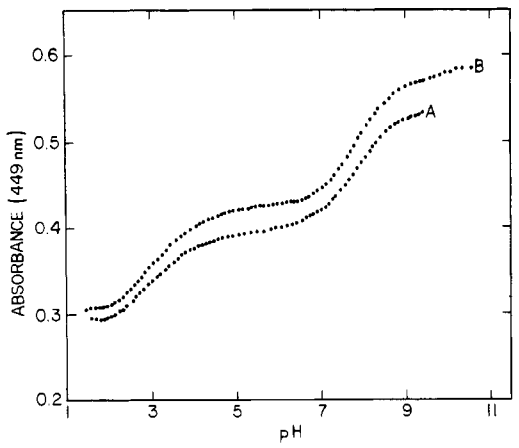

FIGURE 7: Spectrophotometric titration of 1-α-ANP RNase A in the presence of absence of 3′-CMP. (A) 1-α-ANP RNase A, 1.04×10^{-4} M, λ = 449 nm, 25 °C; (B) 1.04×10^{-4} M protein plus 0.01 M 3′-CMP, λ = 449 nm, 25 °C. The solvent was 0.13 M NaCl.

complex (Ettinger & Hirs, 1968) and 17 times larger than that for the dissociation of the 41-DNP RNase A–3′-CMP complex (Ettinger & Hirs, 1968).

The molar difference extinction coefficient at 450 nm is 548 ± 4 M^{-1} cm^{-1}. The lowered affinity of 3′-CMP for 41-ANP RNase A compared to RNase A and 41-DNP RNase A is undoubtedly related to the stabilizing influence of the dianionic ANP group at the active site. In addition to the reduction in binding strength which results from removal of the positive charge on Lys-41 as in 41-DNP RNase A, a further weakening of 3′-CMP affinity occurs in 41-ANP RNase A because the negatively charged arsonate dianion effectively removes additional positive charge from the nucleotide-binding site.

The ANP chromophore is a versatile spectrophotometric probe of the surface structure of RNase A. The group can be introduced selectively into RNase A and perhaps into other anion-binding proteins. Attachment of the ANP group to a lysine residue which constitutes part of a positive center on a protein surface should demonstrate enhanced kinetic selectivity as a result of the dianionic character of ANFB at pH 8. The ANP group monitors structural changes in surface regions with which it is covalently linked. These changes may be induced by ligand binding, acid and thermal denaturation, and chemical modifications. Technical difficulties usually associated with low values of $\Delta\epsilon$ for reporter group chromophores are nonexistent for the ANP moiety for which changes in $\Delta\epsilon$ sometimes exceed 50% of ϵ_{max} values. It is proposed that this reagent may be generally useful in investigating protein–protein or protein–ligand interactions which have an electrostatic basis for the favorable binding.

Acknowledgments

We gratefully acknowledge the technical assistance of Harvey Morrison, Evelyn Hwang, and Thea Weiss. We are indebted to Dr. M. Pincus for reading and critically evaluating the manuscript.

References

Anderson, D. G., Hammes, G. G., & Waltz, F. G., Jr. (1968) *Biochemistry 7*, 1637.

Burr, M., & Koshland, D. E., Jr. (1964) *Proc. Natl. Acad. Sci. U.S.A. 64*, 1017.

Carty, R. P., & Hirs, C. H. W. (1968) *J. Biol. Chem. 243*, 5244.

Cathou, R. E., & Hammes, G. G. (1965) *J. Am. Chem. Soc. 87*, 4674.

Crestfield, A. M., Stein, W. H., & Moore, S. (1963) *J. Biol. Chem. 238*, 2413.

Ettinger, M. J., & Hirs, C. H. W. (1968) *Biochemistry 7*, 3374.

French, T. C., & Hammes, G. G. (1965) *J. Am. Chem. Soc. 87*, 4669.

Friedman, B. E., Olson, J. S., & Matthews, K. S. (1976) *J. Biol. Chem. 251*, 1171.

Garel, J. R. (1976) *Eur. J. Biochem. 70*, 179.

Garel, J. R., & Baldwin, R. L. (1975) *J. Mol. Biol. 94*, 621.

Gorenstein, D. G., & Wyrwicz, A. (1973) *Biochem. Biophys. Res. Commun. 54*, 976.

Hammes, G. G., & Schimmel, P. R. (1965) *J. Am. Chem. Soc. 87*, 4665.

Harrison, L. W., & Vallee, B. L. (1978) *Biochemistry 17*, 4359.

Henkart, P. (1971) *J. Biol. Chem. 246*, 2711.

Hirs, C. H. W., & Kycia, J. H. (1965) *Arch. Biochem. Biophys. 111*, 223.

Hirs, C. H. W., Halmann, M., & Kycia, J. H. (1962) *Biol. Struct. Funct., Proc. IUB/IUBS Int. Symp., 1st, 1960 1*, 41–57.

Hirs, C. H. W., Halmann, M., & Kycia, J. H. (1965) *Arch. Biochem. Biophys. 111*, 209.

Horton, H. R., & Koshland, D. E., Jr. (1967) *Methods Enzymol. 11*, 556.

Horton, H. R., & Koshland, D. E., Jr. (1972) *Methods Enzymol. 25*, 468.

Izatt, R. M., & Christensen, J. J. (1968) in *Handbook of Biochemistry* (Sober, H. A., Ed.) p J-64, The Chemical Rubber Publishing Co., Cleveland, OH.

Johansen, J. T., & Vallee, B. L. (1971) *Proc. Natl. Acad. Sci. U.S.A. 68*, 2532.

Kagan, N. M., & Vallee, B. L. (1969) *Biochemistry 8*, 4223.

Klotz, I. M., & Tosi, L. (1962) *Biochim. Biophys. Acta 63*, 33.

Kortum, G., Vogel, W., & Andrussow, K. (1961) in *Dissociation Constants of Organic Acids in Aqueous Solution*, pp 492–501, Butterworths, London.

Lindquist, R. N., Lynn, J. L., Jr., & Lienhard, G. E. (1973) *J. Am. Chem. Soc. 95*, 8762.

Loeb, G. I., & Saroff, H. A. (1964) *Biochemistry 3*, 1819.

Lowry, O. H., Rosebrough, N. J., Farr, A. L., & Randall, R. J. (1951) *J. Biol. Chem. 193*, 265.

Meadows, D. H., Roberts, G. C. K., & Jardetzky, O. (1969) *J. Mol. Biol. 45*, 491.

Muhlrad, A., Lamed, R., & Oplatka, A. (1975) *J. Biol. Chem. 250*, 175.

Naik, V. R., & Horton, H. R. (1973) *J. Biol. Chem. 248*, 6709.

Patel, D. J., Caruel, L. L., & Bovey, F. A. (1975) *Biopolymers 14*, 987.

Pincus, M., & Carty, R. P. (1970) *Biochem. Biophys. Res. Commun. 38*, 1049.

Pincus, M., LeThi, L., & Carty, R. P. (1975) *Biochemistry 14*, 3653.

Ralston, M. (1977) in *BMDP-77 Biomedical Computer Programs P-Series* (Dixon, W. J., & Brown, M. B., Eds.) pp 484–520, University of California Press, Berkeley, CA.

Ramachandran, L. K., & Sastry, L. V. S. (1962) *Biochemistry 1*, 75.

Shrager, R. I., Cohen, J. S., Heller, S. R., Sachs, D. H., & Schechter, A. N. (1972) *Biochemistry 11*, 541.

Tawada, K., Asai, H., & Gerber, B. R. (1969) *Biochim. Biophys. Acta 194*, 486.

Tsong, T. Y., Hearn, R. P., Wrathall, D. P., & Sturtevant, J. M. (1970) *Biochemistry 9*, 2666.
Ukita, T., Waku, K., Irie, M., & Hoshino, O. (1961) *J. Biochem. (Tokyo) 50*, 405.
Wyckoff, H. W., Tsernoglou, D., Hanson, A. W., Knox, J. R., Lee, B., & Richards, F. M. (1970) *J. Biol. Chem. 245*, 305.
Yagisawa, S. (1975) *J. Biochem. (Tokyo) 77*, 605.
Yang, D. S., & Matthews, K. S. (1976) *J. Mol. Biol. 103*, 433.

Fluorescent-Labeled Cross-Links in Collagen: Pyrenesulfonylhydrazine†

Eiji Fujimori* and Nathaniel Shambaugh

ABSTRACT: Aldol condensation products of two lysyl-derived aldehyde (allysine) residues are involved in cross-linking of collagen. However, the distribution of these cross-links and their age-related changes remain largely unanswered. We have found that the unsaturated aldehydes of aldol condensation cross-links can be fluorescent labeled. When labeled with pyrenesulfonylhydrazine, pyrene dimers and excimers fluoresce at 383 and 485, nm, respectively. (The pyrene dimer is stable in benzene, whereas in polar solvents it exhibts an exponential decay to monomer fluorescing at 378 nm.) Dimers bound to collagen also decay to monomers, but at a more complicated, nonexponential rate. This dissociation in collagen is also associated with gradual decrease in the excimer fluorescence. While dissociated monomers appear to be reassociated by redialysis, the excimer is not regenerated. During fibril formation in vitro of the labeled collagen, two fluorescence changes take place: a very rapid decrease of the excimer fluorescence and a gradual increase of the monomer fluorescence. These changes indicate very early and early conformational changes at the nonhelical terminal telopeptides. The excimer fluorescence also decreases upon thermal and guanidine denaturation. Two different environments for excimer formation are suggested by the latter. It is concluded that pyrenesulfonylhydrazine offers a unique and sensitive probe for the proximity of aldehyde groups as well as for the mobility and conformation changes of the telopeptides in collagen.

In a previous study on the fluorescent labeling of acid-soluble type I collagen with pyrenebutyrylhydrazine (PBH),[1] we have shown the formation of excimer fluorescence, indicating the presence of two adjacent pyrene labels bound to the same collagen molecule (Shambaugh & Fujimori, 1981). Most pyrene molecules were at the nonhelical terminal telopeptides. Unsaturated aldehydes of aldol condensation cross-links in the β chain of collagen (Bornstein & Traub, 1979) were labeled with the pyrene groups. Thus, excimer formation indicated the proximity of two unsaturated aldehydes in collagen.

In the present study, another pyrene derivative, PSH,[1] has been found to have unique characteristics distinct from those of PBH. The solubility of PSH in aqueous solution is higher than that of PBH. The pyrene aggregate fluorescence observed in the PBH–collagen complex is not prominently formed in the PSH–collagen complex. Instead, PSH forms pyrene ground-state dimers which are gradually dissociated to monomers in aqueous solution. In order to obtain more information concerning the proximity of unsaturated aldehydes and the structural changes in the telopeptide, further research has been conducted to investigate PSH excimer formation and related phenomena in collagen. This paper describes the pronounced formation of excimer fluorescence by labeling of collagen with PSH dimers as well as changes in excimer fluorescence. In addition, the dissociation and association of the PSH dimer bound to collagen will be reported in connection with their relation to subtle structural changes at the telopeptides.

Materials and Methods

The preparation of acid-soluble type I collagen, from rat tail of young (4–6 weeks) and old (about 2 years) rats, and $NaBH_4$-reduced collagen, as well as pepsin treatment, was performed as previously described (Crabtree & Fujimori, 1980; Shambaugh & Fujimori, 1981). A small amount of PSH crystals (Molecular Probes, Inc.) was added to 0.2% collagen in 0.005 M acetic acid and stirred at 4 °C overnight. Subsequently, the mixtures were centrifuged twice at 55000*g* for 45 min and dialyzed extensively against 0.005 M acetic acid.

Fluorescence and excitation spectra were measured on a Perkin-Elmer fluorescence spectrophotometer, Model 650-10S, equipped with a temperature-controlled cell holder. A Cary 15 spectrophotometer was used to measure absorption spectra. Fibril formation and gel-filtration experiments were also carried out as previously described (Shambaugh & Fujimori, 1981).

Results

Figure 1 shows the fluorescence and excitation spectra of the freshly prepared PSH–young collagen complex, measured immediately after extensive dialysis against 0.005 M acetic acid. When excited at 330 nm, structural fluorescence bands were at 383, 402, and 425 nm, and an excimer fluorescence appeared at about 485 nm (Figure 1, curve A). Excitation at 360 nm gave rise to increased fluorescence bands (Figure 1, curve B) compared to those excited at 330 nm. The excitation spectrum for the 383-nm fluorescence exhibited maxima at 356 and 363 nm with a shoulder at 340 nm (Figure 1, curve C). These fluorescence and excitation maxima were entirely different from those of a pyrene monomer (see below), indicating that the emitting species is not a monomeric pyrene. Another maximum at about 380 nm was present in the excitation spectrum for the second fluorescence band at 402 nm (not shown). The excitation spectrum for the excimer fluorescence at 485 nm showed two peaks at 360 and 384 nm

† From the Department of Fine Structure, Boston Biomedical Research Institute, Boston, Massachusetts 02114. *Received October 3, 1980.* This study was supported by Research Grant AG00296 from the National Institutes of Health.

[1] Abbreviations used: PBH, pyrenebutyrylhydrazine; PSH, pyrenesulfonylhydrazine.

0006-2960/81/0420-4852$01.25/0